NIH Public Access
Author Manuscript
Stem Cells. Author manuscript; available in PMC 2016 January 01.

Published in final edited form as:
Stem Cells. 2015 January ; 33(1): 253–264. doi:10.1002/stem.1846.

NTPDase2 and Purinergic Signaling Control Progenitor Cell Proliferation in Neurogenic Niches of the Adult Mouse Brain

Kristine Gampe[a,*], **Jennifer Stefani**[a,*], **Klaus Hammer**[a], **Peter Brendel**[a], **Alexandra Pötzsch**[a], **Grigori Enikolopov**[b], **Keiichi Enjyoji**[c], **Amparo Acker-Palmer**[a], **Simon C. Robson**[c], and **Herbert Zimmermann**[a]

[a]Institute of Cell Biology and Neuroscience, Goethe-University, Frankfurt, Germany

[b]Cold Spring Harbor Laboratory, Cold Spring Harbor, NY 11724, USA

[c]Beth Israel Deaconess Medical Center, Division of Gastroenterology, Harvard Medical School, Boston, MA, USA

Abstract

Nerve cells are continuously generated from stem cells in the adult mammalian subventricular zone (SVZ) and hippocampal dentate gyrus. We have previously noted that stem/progenitor cells in the SVZ and the subgranular layer (SGL) of the dentate gyrus express high levels of plasma membrane-bound nucleoside triphosphate diphosphohydrolase 2 (NTPDase2), an ectoenzyme that hydrolyzes extracellular nucleoside di- and triphosphates. We inferred that deletion of NTPDase2 would increase local extracellular nucleoside triphosphate concentrations perturbing purinergic signaling and boosting progenitor cell proliferation and neurogenesis. Using newly generated mice globally null for *Entpd2*, we demonstrate that NTPDase2 is the major ectonucleotidase in these progenitor cell rich areas. Using BrdU-labeling protocols, we have measured stem cell proliferation and determined long term survival of cell progeny under basal conditions. Brains of *Entpd2* null mice revealed increased progenitor cell proliferation in both the SVZ and the SGL. However, this occurred without noteworthy alterations in long-term progeny survival. The hippocampal stem cell pool and the pool of the intermediate progenitor type-2 cells clearly expanded. However, substantive proportions of these proliferating cells were lost during

Corresponding author: Kristine Gampe, Institute for Cell Biology and Neuroscience, Molecular and Cellular Neurobiology, Goethe University, Max-von-Laue-Str. 13, Frankfurt am Main, Germany Tel: +49-69-79842002, Fax: +49-69-79842021, k.gampe@bio.uni-frankfurt.de.
*Kristine Gampe and Jennifer Stefani have equally contributed to the paper.

DISCLOSURE OF POTENTIAL CONFLICTS OF INTEREST
The authors indicate no potential conflicts of interest

Author contribution summary:
Kristine Gampe: Conception and design, collection and assembly of data, data analysis and interpretation, manuscript writing
Jennifer Stefani: Conception and design, collection and assembly of data, data analysis and interpretation
Klaus Hammer: Collection and assembly of data, enzyme histochemistry
Peter Brendel: Collection and assembly of data, in vitro experiments
Alexandra Pötzsch: Collection and assembly of data, progenitor cell expansion
Grigori Enikolopov: Collection and assembly of data, generation of EGFP-nestin mice
Keiichi Enjyoji: Collection and assembly of data, generation of NTPDase2 knockout mice
Amparo Acker-Palmer: Manuscript writing, financial support
Simon C. Robson: Collection and assembly of data, generation of NTPDase2 knockout mice, editing of manuscript
Herbert Zimmermann: Conception and design, data analysis and interpretation, manuscript writing

NIH-PA Author Manuscript
NIH-PA Author Manuscript
NIH-PA Author Manuscript

NIH-PA Author Manuscript

NIH-PA Author Manuscript

NIH-PA Author Manuscript

expansion at around type-3 stage. Cell loss was paralleled by decreases in CREB phosphorylation in the doublecortin-positive progenitor cell population and by an increase in labeling for activated caspase-3 levels. We propose that NTPDase2 has functionality in scavenging mitogenic extracellular nucleoside triphosphates in neurogenic niches of the adult brain, thereby acting as a homeostatic regulator of nucleotide-mediated neural progenitor cell proliferation and expansion.

Keywords

Adenosine 5′-triphosphate; Adult neurogenesis; Ectonucleotidase; Hippocampus; Neural stem cell; Proliferation; Subventricular zone

INTRODUCTION

In the adult mammalian brain, neurons are continuously generated de novo from stem cells in two major neurogenic niches: the subventricular zone (SVZ) of the lateral ventricles and the hippocampal dentate gyrus [1, 2]. The principal mechanisms of neurogenesis in the two brain regions are comparable but also differ in several respects. Specifically, neural stem cells of the SVZ generate neurons for the olfactory bulb. There is strong experimental evidence that the astrocyte-like B cells (or at least a subpopulation) represent the primary neural stem cells, from which the rapidly proliferating C cells and the neurally determined A cells (neuroblasts) are formed. Neuroblasts enter the rostral migratory stream (RMS) and migrate towards the olfactory bulb where they can differentiate into interneurons [3]. Stem cells in the adult hippocampus (type-1 cells) give rise to granule cells of the dentate gyrus. Their cell bodies are situated in the subgranular layer (SGL) and initially generate the strongly proliferating type-2 cells. These in turn generate type-3 cells that migrate at short distance into the granule cell layer, become postmitotic and grow dendrites and an axon [4].

Adult neurogenesis in the olfactory bulb has been related to odor memory and perception [5] whereas neurogenesis in the dentate gyrus is important for hippocampus-specific learning and memory [2]. Several factors, including growth factors and neurotransmitters contribute to proliferation, neuronal integration and/or survival [6, 7]. To date little is known how the lifetime of the various signal substances is controlled and how homeostasis of the neurogenesis pathway is maintained.

Increasingly new data indicate that extracellular purine and pyrimidine nucleotides are involved in the control of both embryonic and adult neurogenesis. These extracellular nucleotides act via ionotropic P2X or metabotropic P2Y receptors. ATP was found to be released from cultured SVZ-derived neural progenitors [8], from B1 cells in acute brain slices [9] and from hippocampal astrocytes [10]. Several studies provided evidence that ATP or UTP stimulate proliferation or also migration of embryonic or adult neural progenitor cells in vitro [8, 11–14].

Work on rat and mouse embryonic brain slices further revealed that neural precursors in situ could release ATP. Extracellular ATP induces receptor-mediated Ca^{2+} fluctuations in ventricular zone precursors and facilitates progenitor cell proliferation and migration within the developing cortex [15–17]. Additional studies on the adult SVZ [18] or the adult

NIH-PA Author Manuscript

NIH-PA Author Manuscript

NIH-PA Author Manuscript

hippocampus [10, 19] in situ or on organotypic cultures of the SVZ [20] further provide evidence that ATP or the ADP analog adenosine 5′-O-2-thiodiphosphate (ADPβS) can promote progenitor cell proliferation in the adult.

The functionality of extracellular nucleotides is controlled by ectonucleotidases, which are plasma membrane-bound enzymes, of which the catalytic site faces the cell exterior [21]. We have previously shown that the extracellular nucleotide hydrolyzing enzyme nucleoside triphosphate diphosphohydrolase2 (NTPDase2) is highly expressed on adult neural progenitor cells (B cells) of the SVZ and RMS [22] and on type-1 to type-3 cells of the hippocampus but is absent from stellate astrocytes or mature neurons [23]. NTPDase2 catalyzes the dephosphorylation of nucleoside triphosphates, generates nucleoside diphosphates and eventually the respective nucleoside monophosphates, thus terminating their effect on nearby nucleotide receptors.

We have hypothesized that NTPDase2 plays a major role in controlling the impact of extracellular nucleotides in these major neurogenic niches. In turn, deletion of the enzyme would be expected to have a major impact on extracellular nucleotide-mediated functions that in turn influence adult neurogenesis. We analyzed an *Entpd2* null mouse model [24] to obtain in situ information on the functional role of nucleotides on progenitor cell proliferation and neuron formation in the non-injured SVZ and hippocampus. Our results suggest that NTPDase2 functions to modulate nucleotide-mediated progenitor cell proliferation and expansion, thereby acting as a homeostatic regulator of nucleotide-mediated neural progenitor cell proliferation and expansion under basal conditions.

MATERIALS AND METHODS

Animals

All animal experiments were approved by the local government and conducted under veterinary supervision in accordance with European regulations. Experiments were performed using mice aged 8–12 weeks. Animals were kept under 12 hours light and dark cycle with food and water ad libitum. *Entpd2* null and other mutant mice with the corresponding wild types (litters) were bred in house.

Entpd2 targeting was initiated at BIDMC, Harvard University, Boston (SCR/KE) where constructs to generate null mice were designed to delete Exons I and II, including the entire promoter region. *Entpd2* KO animals were then generated by homologous recombination in murine ES cells derived from 129Sv at GenOway, Lyon, France (www.genoway.com). The resultant mutant mice were screened by PCR and homozygous *Entpd2* mice were created, in which the gene deletion was validated by PCR and immunohistochemistry. To identify primary neural stem cells in the neurogenic niches, we bred mice expressing the enhanced green fluorescent protein (EGFP) under control of the nestin promoter [25] to *Entpd2* KO mice. Gene deletions and nestin-driven EGFP expression were confirmed by immunohistochemistry and genotyping of 3–4 week old pubs using oligonucleotides given in Table S1. For analysis of progenitor cell proliferation and survival mice received 5 daily intraperitoneal injections of the thymidine analogue 5-bromo-2-deoxyuridine (BrdU; 50

NIH-PA Author Manuscript

NIH-PA Author Manuscript

NIH-PA Author Manuscript

mg/kg of body weight, Sigma-Aldrich, Steinheim, Germany, www.sigmaaldrich.com). Animals were perfused either 2 hours or 4 weeks after the final BrdU pulse.

For analysis specifically of type-1 cell proliferation, mice received 3 intraperitoneal BrdU injections at 2 hour interval. Animals were perfused 2 hours after the final BrdU pulse.

Enzyme Histochemistry

For histochemical analysis of neurogenic niches animals received an anaesthetic overdose of ketamine (100 mg/kg body weight; Ketavet, Pfizer Pharmacia, Berlin, Germany), xylazine (10 mg/kg body weight; Rompun, Bayer Vital, Leverkusen, Germany) and pentobarbital (20 mg/kg body weight; Narcorene, Merial GmbH, Hallbergmoos, Germany) and were intracardially perfused with 10 ml of physiological saline (0.9% NaCl) followed by perfusion with 150 ml of ice-cold 4% paraformaldehyde in phosphate-buffered saline (PBS: 137 mM NaCl, 2.7 mM KCl, 10.1 mM NaHPO4, 1.8 mM KH_2PO4, pH 7.4). Brains were isolated, postfixed overnight in 4% paraformaldehyde/PBS and cryoprotected with 30% sucrose/PBS for 24 hours to 48 hours at 4°C. After embedding in Tissue-Tek (Sakura, Staufen, Germany, www.sakuraeu.com), brains were frozen and serially cut into 40 μm thick sagittal or coronal floating sections, using a Leica microtome (CM 3050S, Leica, Wetzlar, Germany, www.leica-microsystems.com).

ATPase, ADPase, and AMPase activity was visualized as previously described [26]. In brief, cryosections were preincubated for 30 min at room temperature with Tris-maleate sucrose buffer (TMS; 0.25 M sucrose, 50 mM Tris-maleate, pH 7.4) containing 2 mM $MgCl_2$. The enzyme reaction was performed at 37°C in TMS-buffered substrate solution [2 mM $Pb(NO_3)_2$, 5 mM $MnCl_2$, 2 mM $MgCl_2$, 50 mM Tris-maleate, pH 7.4, plus 0.25 M sucrose stabilized with 3% dextran T 250 (Roth, Karlsruhe, Germany, www.carlroth.com)] for 30 min, containing 1 mM of either of the following substrates: ATP, ADP (both Sigma-Aldrich), AMP (Boehringer, Ingelheim, Germany, www.boehringer-ingelheim.com). After rinsing with demineralized water the lead orthophosphate precipitated as a result of nucleotidase activity was visualized as a brown deposit by incubating sections in an aqueous solution of 1% (v/v) $(NH_4)_2S$. For detection of alkaline phosphatase activity the BCIP/NBT system (Sigma-Aldrich) was applied according to the manufacturer's protocol. Sections were dehydrated in graded ethanol and mounted with Roti-Histokit II (Roth).

Immunocytochemistry

For detection of overall BrdU labeling in SVZ and hippocampus, floating sections (40 μm) were pretreated with 0.6% H_2O_2 in Tris-buffered saline (TBS; 0.15 M NaCl, 0.1 M Tris-HCl, pH 7.5) for 30 min to denature DNA, rinsed in TBS and incubated in 50% formamide in 2x saline-sodium citrate buffer (SSC) (0.3 M NaCl, 0.03 M sodium citrate) at 65°C for 2 hours followed by a 5-minute rinse in 2x SSC and a 30-minute incubation in 2 M HCl at 37°C. Sections were neutralized by incubation in 0.1 M boric acid for 10 min, washed in TBS and blocked with 3% normal donkey serum in TBS containing 0.1 % Triton-X-100 for 30 min, followed by incubation with an anti-BrdU antibody (AbD Serotec, Düsseldorf, Germany, www.abdserotec.com) in the same blocking solution (overnight at 4°C). Following several rinses in TBS, sections were incubated for 1 hour with secondary

NIH-PA Author Manuscript

NIH-PA Author Manuscript

NIH-PA Author Manuscript

antibodies (Biotin-coupled donkey anti-rat, Cy3-coupled donkey anti-mouse, Cy5-coupled donkey anti-rabbit, Dianova, Hamburg, Germany, www.dianova.com) and Alexa fluor 488-coupled donkey anti-rat, Invitrogen, Karlsruhe, Germany, www.lifetechnologies.com) at room temperature. Cryosections were washed in TBS and, in case of peroxidase detection, an avidin-biotin-peroxidase complex (Vector Labs/Biozol, Eching, Germany, www.biozol.de) was applied for 1 hour at room temperature and sections were incubated in diaminobenzidine (DAB) substrate solution (25 mg/ml DAB, Sigma-Aldrich, 0.01% H_2O_2, 0.04% NiCl) for 10 min.

For triple fluorescent immunostaining for BrdU and additional antigens, antibodies against the glial fibrillary acidic protein (GFAP, Sigma-Aldrich), NeuN, (Millipore, Schwalbach, Germany, www.millipore.com) or GFP (Abcam plc, Cambridge, UK) the protocol was adapted by omitting incubation with H_2O_2. For standard immunohistochemical procedures the following antibodies were applied: anti-Sox-2 (Y-17, sc-17320, Santa Cruz Biotechnology, Heidelberg, Germany, www.scbt.com), anti-doublecortin (DCX, Santa Cruz Biotechnology), anti-NTPDase2 [22], anti-phospho-CREB (Ser133), and rabbit anti-cleaved caspase-3 (Asp175) (Cell Signaling Technology/New England Biolabs, Frankfurt, Germany, www.cellsignal.com). DNA denaturation was replaced by cell permeabilization with 0.1% Triton-X-100/PBS. Washed cryosections were transferred onto glass slides and mounted in AquaPolymount (Polyscience, Eppelheim, Germany, www.polysciences.com).

Stereological Quantification Procedures

For quantification of peroxidase-labeled BrdU-positive cells, a systematic random counting approach was applied as previously described [27]. Region-specific adaptations from this protocol included 1) for the olfactory bulb: section intervals of 160 µm, a counting frame size of 60 × 60 µm and a counting grid of 250 × 250 µm, 2) for the SVZ: section intervals of 240 µm, a 25 × 25 µm counting frame in a 40 × 60 µm counting grid, and 3) for the hippocampal neurogenic niche: section intervals of 160 µm, without counting frames. The volume of each structure was determined by tracing the areas via a semi-automatic stereology system (Stereoinvestigator, MicroBrightField, Colchester, USA, www.microbrightfield.com). The total number of BrdU-labeled cells per region analyzed was multiplied by the ratio of reference volume to the sampling volume in order to obtain the estimated number of BrdU-positive cells for the entire structure. In order to determine the frequency of newly formed neurons, serial sections spaced 160 µm apart were stained for double immunofluorescence using antibodies against BrdU and NeuN as described above. 50 – 100 BrdU-labeled cells per animal and brain structure were analyzed for marker colocalization, yielding the percentage of the NeuN-expressing BrdU-positive cell population.

For quantification of subtypes of hippocampal progenitor cells (type-1 to type-3) sagittal cryosections from EGFP-expressing WT or *Entpd2* KO mice were immunostained for GFAP, Sox2 and DCX. Similarly, pCREB immunostaining in DCX-immunopositive cells was quantified in sections from WT and *Entpd2* KO mice. Individual sagittal cryosections were assigned to specific brain levels. Four sections with an interspace of 240 µm were

NIH-PA Author Manuscript

NIH-PA Author Manuscript

NIH-PA Author Manuscript

analyzed and cells located within the SGL and up to 10 μm deep into the granule cell layer were included.

For quantification of cells positive for EGFP/GFAP and EGFP/GFAP/BrdU (type-1 cells) located within the SGL (up to 10 μm deep into the granule cell layer) serial sagittal sections spaced 160 μm apart (10 sections per animal) were analyzed.

Cleaved caspase-3 was analyzed in serial coronal sections with an interspace of 160 μm (6 sections per animal). To avoid multiple counts of the identical cell and for quantification of double staining, stacks of ten confocal planes were recorded with a Leica TCS SP5 confocal laser scanning microscope (Leica) and analyzed (interspaces 1 ± 0.05 μm) using Imaris (x64 7.6.1 Bitplane AG, Zurich, Switzerland, www.bitplane.com). All quantification procedures were performed in a double-blinded manner.

Immunoblotting and Quantitative Analysis

Total mouse brain was homogenized and membrane fractions were isolated, taken up in concentrated sample buffer in the absence of reducing agent, run on a 10% Tris-glycine sodium dodecyl sulfate-polyacrylamide gel electrophoresis and transferred onto nitrocellulose membrane (GE Healthcare Life Sciences, Freiburg, Germany, www.gelifesciences.com) using semi-dry blotting techniques (BioRad, Munich, Germany, www.bio-rad.com). Membranes were blocked with 5% skimmed milk powder in PBS containing 0.1% Tween20 (PBS/T) over night at 4°C. Incubation with the primary antibodies anti-TNAP (gift from Yukio Ikehara, Fukuoka, Japan) or anti-NTPDase1–3 (kindly provided by Jean Sévigny, Québec, Canada) was performed overnight at 4°C in PBS/T containing 0.02% NaN_3 and 5% bovine serum albumin followed by incubation with an anti-actin antibody (Sigma-Aldrich) for 1 hour at room temperature. Slices were blocked for 5×10 min with 5% skimmed milk powder, followed by incubation with the respective horseradish peroxidase (HRP)-conjugated secondary antibodies (GE Healthcare) and a final washing step in PBS/T (5×10 min). Immunoblots were incubated with Amersham ECL Western Blotting Detection Reagents and bands were visualized using ImageQuant LAS 4000 (both GE Healthcare). Levels of ectoenzyme immunostaining were standardized to levels of actin immunostaining.

Neurosphere Culture

Preparation of neural progenitors and culture of neurospheres from *Entpd2* WT or KO animals was adapted from [12]. Brains were sliced into 400 μm thick coronal slices with a tissue chopper (anterior-posterior positions 1.2–0.5 mm relative to Bregma). The SVZ was excised from tissue slices in ice-cold PBS buffer. The tissue was enzymatically dissociated with 0.5 mg/ml papain (14 U/mg) dissolved in DMEM/F12 media (Invitrogen) containing 0.1 mM ethylenediaminetetraacetic acid (for 30 min at 37°C). The cell suspension was mixed with the same volume of trypsin ovomucoid inhibitor (0.7 mg/ml in DMEM/F12) containing 1,000 U/ml of DNase I (Sigma-Aldrich). After mechanical dissociation, the cell suspension was centrifuged at 260 g_{av} for 6 min and plated in uncoated dishes in culture media [B27 as supplement, (Invitrogen); DMEM/F12, 10 mM HEPES buffer [pH 7.2], (both PAA Laboratories/GE Healthcare) 100 U/ml penicillin, 10 μg/ml streptomycin (both Sigma-

NIH-PA Author Manuscript

NIH-PA Author Manuscript

NIH-PA Author Manuscript

Aldrich) including 20 ng/ml of human recombinant epidermal growth factor (EGF), 10 ng/ml fibroblast growth factor-2 (FGF-2), (both PeproTech, Hamburg, Germany, www.peprotech.com)].

In vitro Proliferation Studies

After 7 days in vitro, primary neurospheres were dissociated and 5,000 cells/well were replated into 24-well plates in 1 ml of culture medium with 5 ng/ml human recombinant EGF, 2.5 ng/ml FGF-2 as previously described [12]. After 4 days in culture, secondary neurospheres were centrifuged at 260 g_{av} for 6 min, treated with accutase II at 37°C for 45 min and mechanically dissociated. The number of viable cells was counted using a hemocytometer. For experimental rescue of ATPase activity in secondary *Entpd2*−/−neurospheres, apyrase (dissolved in DMEM/F12, 1 U; high ratio A6410; Sigma-Aldrich), heat-inactivated apyrase (95°C, 5 min), or an equal volume of medium was added daily to the culture medium. One preparation of cells with five determinations per condition for each of the studied animals equated to n=1.

Statistical Analysis

Data are presented as mean values ± SEM. Differences between groups were evaluated by the unpaired, two-sided Student's t-test. Differences were considered significant at the 5% level distinguishing significance levels of: * $p \leq 0.05$; ** $p \leq 0.01$; *** $p \leq 0.001$.

RESULTS

Loss of NTPDase2 is not Compensated by Upregulation of other Ectonucleotidases

As depicted by enzyme histochemistry, genetic deletion of *Entpd2* results in a strong reduction of ecto-ATPase catalytic activity in sections of mouse brain. This is particularly obvious in the olfactory bulb, the cerebral cortex, brain stem and molecular layer of the cerebellum (Fig. 1A). Significant reaction product is maintained in the caudoputamen and the substantia nigra. This suggests that NTPDase2 is a major enzyme involved in the hydrolysis of extracellular ATP in mouse brain.

NTPDase2 has a high preference for the hydrolysis of ATP over ADP and it does not hydrolyze AMP [21]. Accordingly, when ADP is used as a substrate, weak enzyme staining remains and *Entpd2* deletion does not cause further substantial reduction. The staining of blood vessels is retained (Fig. 1B). This is due to activity of NTPDase1 that hydrolyzes ATP and ADP about equally well [28]. Hydrolysis of AMP at neutral pH denotes the distribution of ecto-5′-nucleotidase [26]. This enzyme is highly expressed in the caudoputamen. Staining remains unaltered in *Entpd2*-knockout brains (Fig. 1C). Tissue nonspecific alkaline phosphatase (TNAP, the isoform of alkaline phosphatase that hydrolyzes ATP to adenosine in rodent brain, [29]) is expressed throughout the brain but activity at neutral pH is negligible as compared to that of other ectonucleotidases [26]. Enzyme histochemical staining for alkaline phosphatase is not impacted by *Entpd2* deletion (Fig. 1D).

We have previously shown that NTPDase2 is particularly highly expressed by the neural progenitor cells of the hippocampus [23] and the SVZ [22]. This can be depicted by enzyme

NIH-PA Author Manuscript

NIH-PA Author Manuscript

NIH-PA Author Manuscript

histochemical staining with ATP as the substrate (Fig. 1E). Deletion of *Entpd2* results in loss of enzyme staining in the two neurogenic niches with strong biochemical NTPDase activity remaining in the blood vessels. However, there were no apparent changes in overall brain structure.

To further scrutinize the effect of *Entpd2* deletion on the expression of other ATP-hydrolyzing ectonucleotidases we performed quantitative Western Blots of membrane fractions derived from total mouse brain (Fig. 1F). Whereas the immunosignal for NTPDase2 is essentially eliminated, the immunosignals for NTPDase1, NTPDase3 (that also hydrolyze ATP and ADP) and TNAP are unchanged. NTPDase8 is not expressed in rodent brain [30]. These data demonstrate that *Entpd2* deletion does not result in the altered expression of other ectoenzymes capable of hydrolyzing extracellular ATP, ADP or AMP.

Maintenance of Neural Stem Cells in *Entpd2* Knockout Mice

Neural stem cells can no longer be depicted in the knockout animals by ATPase histochemistry (Fig. 1E). We therefore asked whether deletion of *Entpd2* would alter the general structure of these complex cells. For visualizing neural stem cells we crossed mice expressing EGFP under the control of the nestin regulatory elements [25] with *Entpd2* knockout mice. Hippocampal neural stem cells (type-1 cells, [4]) reveal an asymmetric shape with the cell body in the SGL of the dentate gyrus, a long apical process traversing the granule cell layer and elaborate bushy ramifications in the internal molecular layer. In WT animals these EGFP-expressing radial cells are immunopositive for NTPDase2 (Fig. 2A).

Following deletion of *Entpd2*, type-1 cells retain their typical polar and ramified structure but immunostaining for NTPDase2 is lost (Fig. 2A). This suggests that deletion of *Entpd2* has no general effect on hippocampal stem cell morphology. Similarly, no apparent alterations were observed in the structure and distribution of nestin-EGFP-positive progenitor cells in the SVZ.

Progenitor Cell Proliferation is Increased in *Entpd2* KO mice

Our results demonstrate that catalytic activity of NTPDase2 is particularly high at the surface of progenitor cells. Deletion of the enzyme should cause an increase in the concentration of extracellular nucleoside triphosphates in the neurogenic niches. We hypothesized that any function these nucleotides play in adult neurogenesis should be enhanced in the *Entpd2* KO mice.

We therefore investigated the effect of *Entpd2* deletion on progenitor cell proliferation and long-term cell survival in both the SVZ and the dentate gyrus. Mice received five daily intraperitoneal BrdU injections. They were perfused either 2 hours or 4 weeks after the final BrdU pulse. Quantitative evaluation of the immunostained BrdU-positive cells 2 hours after the final BrdU pulse revealed an increase in cell number in the SVZ of 154% (Fig. 2B,D) and of 81% in the SGL of the dentate gyrus (Fig. 2F,H). This suggests that NTPDase2 functions as a brake on nucleotide-mediated cell proliferation in either neurogenic niche. After four weeks, BrdU-labeled cells had migrated to the olfactory bulb or into the granule cell layer of the hippocampus and had either undergone apoptosis or had differentiated into

NIH-PA Author Manuscript

NIH-PA Author Manuscript

NIH-PA Author Manuscript

interneurons [3]. No difference was observed between WT and KO mice in the number of BrdU-positive cells in the olfactory bulb (Fig. 2C,E) or in the hippocampal SGL (Fig. 2G,I). These data suggest that deletion of NTPDase2 results in an increase in neural progenitor cells. However, the surplus of cells is subsequently lost. This notion is further supported by the lack of significant difference between WT and KO animals in the volumes (WT versus KO, mm^3) of the granule cell layer (0.27±0.01 versus 0.26±0.01), the molecular layer (0.77 ± 0.04 versus 0.75 ± 0.03), hilus (0.24 ± 0.05 versus 0.20 ± 0.01) or entire dentate gyrus (1.28 ± 0.09 versus 1.21 ± 0.05) (all means ± S.E.M., n=5–10).

Excessive Progenitors do not Form more Neurons

To compare the extent of neuron formation we determined the contribution of NeuN-positive cells to the total of BrdU-positive cells surviving after four weeks. In the olfactory bulb, we separately analyzed the granule cell layer and the glomerular layer, both major targets of SVZ-derived progenitors [31]. In the granule cell layer of the olfactory bulb 92% of all BrdU-labeled cells were found to be immunopositive for NeuN, revealing that almost all of the labeled progenitor cells had become neurons and that there is no difference between KO and WT mice (Fig. 3A,B). In contrast, the contribution of labeled NeuN-positive cells in the glomerular layer was only between 45% and 53% in WT and KO, respectively (Fig. 3C,D). In the hippocampal granule cell layer the contribution of labeled NeuN-positive cells was around 83% for both genotypes (Fig. 3E,F). In either case there was no significant difference between WT and KO mice. These results suggest that the extent of nerve cell formation is not altered in *Entpd2* KO mice.

The Hippocampal Progenitor Pool is Expanded in *Entpd2* KO mice

Our results implicated that *Entpd2* deletion increases progenitor cell proliferation. But at the same time homeostatic mechanisms would prevent an increase in new neuron formation. This raised the question at what stage of the differentiation cascade progenitor cells are eliminated. We compared the abundance of individual progenitor cell types between WT and KO animals. To ease the identification of type-1 cells we again relied on *Entpd2* KO mice expressing nestin-EGFP. The following stages were differentiated on the basis of immunostaining [4, 32]: type-1 (expressing nestin-EGFP, GFAP and the transcription factor Sox2), type-2a (expressing nestin-EGFP and Sox2), type-2b (expressing nestin-EGFP and the microtubule-associated protein DCX), type-3+ (immunopositive for DCX but lacking the other markers) (Fig. 4A,B). The dense spacing of nestin-EGFP-, GFAP- and Sox2-positive cells in the SGL made it difficult to distinguish individual cells. For this reason only cells with at least a short process (facing the granule cell layer), typical of type-1 cells, were counted. Type-3+ cells include type-3 cells as defined by [4] as well as any DCX-positive cells that may in addition express the neuronal marker NeuN that is increasingly expressed with structural maturation of DCX-positive cells [33]. We found an increase in 33% in the number of type-1 cells in the *Entpd2* KO mice. Similarly, the number of type-2a and type-2b cells was increased (by 23% and 29%, respectively) whereas the number of type-3+ cells was unaltered (Fig. 4C). To corroborate the expansion of the type-1 cell pool we counted in addition in the same sections the number of nestin-EGFP-positive cells with a radial process traversing the entire granule cell layer. Cell numbers (four sections per animal) were

NIH-PA Author Manuscript

NIH-PA Author Manuscript

NIH-PA Author Manuscript

increased form 169.7 ± 14.5 in the WT to 219.4 ± 11.5 in the *Entpd2* KO mice corresponding to an increase in 29.3% (mean ± SEM, n= 9, p=0.004).

We further investigated whether type-1 cells in the adult *Entpd2* KO mice might undergo enhanced levels of proliferation. Two hours after three consecutive intraperitoneal BrdU injections at 2 hours interval BrdU incorporation into EGFP/GFAP-positive cells (type-1 cells) was quantified. Fig. 4D depicts examples of BrdU-labeled cells. In analogy to the previous series of experiments (comp. Fig. 4C) the total number of type-1 cells was increased in the KO animals (26%) (Fig. 4E). Notably, the contribution of BrdU-labeled type-1 cells was disproportionally increased by 62% in the *Entpd2* KO mice (Fig. 4F). Whereas in WT animals 4.4% of all type-1 cells had incorporated BrdU it was 5.6% in the KO animals. This corresponds to an increase of 27% in overall BrdU labeling of type-1 cells in *Entpd2* KO mice.

Increased apoptosis in *Entpd2* KO mice

As the hippocampal pool of progenitor cells is initially increased in the KO mice but more mature cell numbers are noted in WT mice, one would expect increased apoptosis in the mutant mice. It has previously been reported that apoptotic cells in the SGL are rapidly removed by microglia [34] and as a consequence the incidence of apoptotic cells is low in the SGL. We applied immunostaining for cleaved caspase-3 to compare the extent of apoptosis between KO mice and WT control. Apoptotic cells were observed exclusively in the SGL (Fig. 5A) and their number was increased by a factor of approximately 2.5 in the KO mice (Fig. 5B).

CREB Phosphorylation is Decreased in DCX-Expressing Cells

It has previously been reported that in the adult dentate gyrus pCREB is preferentially located to DCX-expressing cells [35] and that loss of CREB phosphorylation compromises the survival of newborn neurons [36]. We therefore compared the extent of CREB-phosphorylation in DCX-immunopositive cells between WT and KO animals (Fig. 5C,D). The total number of DCX-immunopositive cells was identical in WT and KO animals. However, in *Entpd2* KO mice immunostaining for pCREB in DCX-positive cells was decreased by 30% (Fig. 5D). Together these data suggest that the pool of type-1 neural stem cells and their derivatives type-2a and type-2b is expanded in *Entpd2* KO animals but that around stage 3+ the pool is reduced to WT control. The decrease in CREB phosphorylation of type-3+ cells further supports the notion that these cells lose responsiveness to survival factors.

Progenitor Cell Proliferation is also Increased in vitro

In order to investigate whether deletion of *Entpd2* also leads to increased cell proliferation in vitro we analyzed cell numbers in primary and secondary neurospheres. In the knockout animals cell number was increased by 46% and 79%, respectively (Fig. 5A,B). If an increase in extracellular nucleotide concentrations was responsible for the increased cell proliferation in neurospheres from *Entpd2* KO mice, addition of the ATP/ADP-hydrolyzing enzyme apyrase to the neurospheres should cause a reduction. Apyrase reduced the number of neurosphere cells derived from *Entpd2* KO mice to 71%, as compared to an equal volume of

NIH-PA Author Manuscript

NIH-PA Author Manuscript

NIH-PA Author Manuscript

culture medium. The addition of heat-inactivated apyrase had no effect on cell numbers (Fig. 5C). This further supports the notion that deletion of *Entpd2* increases extracellular nucleotide concentrations and nucleotide-mediated constitutive enhancement of adult neural progenitor cell proliferation via P2-receptor signaling.

DISCUSSION

The major result in this study is that deletion of the ectonucleotidase NTPDase2 results in increased progenitor cell proliferation in both the SVZ and the SGL of the dentate gyrus. This suggests that NTPDase2 is functional in controlling extracellular nucleotide concentrations in the neurogenic niches thereby acting as a homeostatic regulator of neural progenitor cell proliferation and expansion.

Deletion or knockdown of *Entpd2* was previously shown to reduce extracellular ATP hydrolysis and to increase extracellular ATP concentrations [24, 37]. Similarly, inhibition of ectonucleotidase activity by the NTPDase inhibitor PV4 in rat striatum resulted in an increase of resting extracellular ATP concentrations from 40 nM to 360 nM [38].

In vitro studies demonstrate that agonists of several nucleotide receptors such as P2Y1 (responding to ATP and ADP), P2Y2 (responding to ATP and UTP), and also P2Y13 (responding to ADP) can elevate intracellular Ca^{2+} concentrations in neural progenitor cells, induce intracellular signaling pathways involved in cell proliferation or stimulate progenitor cell proliferation [8, 11, 12, 14, 39]. P2Y1 receptor-mediated increases in intracellular Ca^{2+} have been observed in B cells in acute slices of the mouse SVZ [40]. Moreover, recent in vivo studies with ventricular infusion of ATP and analysis of *P2ry1* KO mice [18] or of infusion with ADPβS [19] suggest that P2Y1 receptors can enhance progenitor cell proliferation in the SVZ in situ. The presence of P2Y1 receptors in the SVZ has also been demonstrated by in situ hybridization [12]. Evidence from mice lacking the inositol 1,4,5-trisphosphate receptor type-2 supports the notion that also hippocampal progenitor cell proliferation can be enhanced by P2Y1 receptor-mediated purinergic signaling [10].

In addition to the G-protein-coupled P2 receptors, functional ATP-gated ion channels (P2X receptors) have been noted within the neurogenic niches. This includes a non-specified P2X receptor in nestin-GFP-positive adult hippocampal progenitors [23] and the P2X7 receptor in nestin-EGFP-positive precursor cells of the mouse SVZ [41]. A slight increase in BrdU incorporation of the hippocampal granule cell layer was observed in *P2rx7* KO mice [42] and non-specified P2X receptors have been inferred in the stimulation of BrdU incorporation in the SVZ of organotypic brain cultures from P15 mice [20]. In contrast, in cultured fetal [43] or adult [41] neural progenitor cells activation of the P2X7 receptor induced cell death. Together, this evidence suggests that nucleotides can act as important mediators in the two neurogenic niches via a variety of P2 receptors.

Our data further show that increased progenitor cell proliferation is not necessarily directly coupled to increased neuron formation. While surplus generation and later selection for long-term survival is a general principle of hippocampal neurogenesis [44], specific albeit potentially redundant mechanisms must exist that tightly regulate and maintain homeostasis

NIH-PA Author Manuscript

NIH-PA Author Manuscript

NIH-PA Author Manuscript

of the pool of newly generated neurons. This concerns the regulation of progenitor cell proliferation as well as of cell survival and neuronal differentiation. In the case of nucleotides NTPDase2 would subserve this function.

Differential effects on hippocampal progenitor cell proliferation and cell survival were observed between behavioral paradigms. Whereas living in enriched environment only affected cell survival, but not cell proliferation, running increased both proliferation and net neuronal survival [45, 46]. Exercise-induced secretion of growth factors such as BDNF [47] or enriched excitatory input to the neuronal precursor cells and new circuit construction [48, 49] may enforce the pro-neurogenic pathway – which may be missing in the conditions of our experiments. In the olfactory system, proliferation (SVZ and RMS) and neuron formation (olfactory bulb) are spatially separated. Whereas a considerable number of growth factors, hormones and transmitters have been implicated in enhancement of cell proliferation in the SVZ, olfactory learning was found to increase neuron formation in the olfactory bulb [50].

Microglia is involved in apoptotic hippocampal progenitor cell clearance [34]. Microglia phagocytosis is in turn regulated by purinergic signaling [51] and activated by UDP acting via the P2Y6 receptor [52]. NTPDase1, a homolog of NTPDase2 that also hydrolyses nucleoside tri- and diphosphates is expressed by microglia [28]. Its deletion attenuates microglial phagocytosis presumably by preventing the local production of nucleoside diphosphates [53]. Surplus generation of nucleoside triphosphates in the neurogenic niches due to deletion of *Entpd2* and increased NTPDase1-mediated production of UDP at the surface of microglia could be a factor contributing to enhanced progenitor cell clearance.

Single and double nucleotide pulse labeling and lineage tracing experiments suggested that after a few asymmetric divisions neural stem cells convert into astrocytes, resulting in an age-dependent decrease of the hippocampal stem cell pool [54]. In the *Entpd2* KO mice the hippocampal neural stem cell pool was expanded. Furthermore type-1 cells revealed a disproportionally high incorporation of BrdU, reflecting either changes in cell cycle length or increased numbers of proliferating cells. Self-renewal of adult type-1 cells has previously been suggested [55] and social isolation of mice was found to result in the expansion of the hippocampal stem cell pool [56, 57].

Following BrdU application the number of labeled hippocampal progenitors reaches a maximum at about three days and then declines [54, 58]. Our data suggest that the increased BrdU incorporation into the progenitor cell pool of *Entpd2* KO mice is mainly due to enhanced proliferation of type-1 and type-2 cells. Type-3 cells retain the ability to proliferate and transmit to postmitotic maturing granule cells. The majority of cells reach this stage within 3 days [4, 58]. Our observation that the number of type-1 and type-2 cells is constitutively increased in *Entpd2* KO mice but that the number of type-3+ cells is unaltered suggests that in *Entpd2* KO mice the elimination of additional precursors takes place around type-3 stage. The notion that the surplus progenitors in *Entpd2* KO mice are lost at that stage is further supported by our observation that apoptosis is increased and that the contribution of DCX-positive cells containing phosphorylated CREB is reduced. CREB phosphorylation closely relates to structural maturation of DCX-positive cells [33]. CREB signaling is of

NIH-PA Author Manuscript

NIH-PA Author Manuscript

NIH-PA Author Manuscript

relevance for survival, maturation and integration of immature (DCX-expressing) neuroblasts but not proliferation of hippocampal progenitors [36].

CONCLUSION

In summary, our data show that NTPDase2 is the major ectonucleotidase within the two major neurogenic niches of the mouse brain. The genetic deletion of this ectoenzyme increases progenitor cell proliferation in either of these niches. NTPDase2 thereby acts to limit constitutive nucleotide-mediated progenitor cell proliferation and expansion under basal conditions. We suggest that NTPDase2 contributes to progenitor cell homeostasis in the neurogenic niches of the adult brain.

Supplementary Material

Refer to Web version on PubMed Central for supplementary material.

Acknowledgments

This work was supported by grants from the Cluster of Excellence EXC 115 and Gutenberg Research College (GCR) Mainz University (to A.A-P) and from NIH P01 HL087203 to SCR.

We would like to thank Jean Sévigny (Laval) for providing NTPDase1 to NTPDase3 antibodies, and Christian Gachet (Strasbourg) for providing *P2ry1* KO mice. This work was supported by grants from the Cluster of Excellence EXC 115 and Gutenberg Research College (GCR) Mainz University (to A.A-P) and from NIH P01 HL087203 to SCR.

References

1. Kriegstein A, Alvarez-Buylla A. The glial nature of embryonic and adult neural stem cells. Annu Rev Neurosci. 2009; 32:149–184. [PubMed: 19555289]
2. Deng W, Aimone JB, Gage FH. New neurons and new memories: how does adult hippocampal neurogenesis affect learning and memory? Nat Rev Neurosci. 2010; 11:339–350. [PubMed: 20354534]
3. Zhao CM, Deng W, Gage FH. Mechanisms and functional implications of adult neurogenesis. Cell. 2008; 132:645–660. [PubMed: 18295581]
4. Kempermann G, Jessberger S, Steiner B, Kronenberg G. Milestones of neuronal development in the adult hippocampus. Trends Neurosci. 2004; 27:447–452. [PubMed: 15271491]
5. Gheusi G, Lledo PM. Adult neurogenesis in the olfactory system shapes odor memory and perception. Prog Brain Res. 2014; 208:157–175. [PubMed: 24767482]
6. Mu YL, Lee SW, Gage FH. Signaling in adult neurogenesis. Curr Opin Neurobiol. 2010; 20:416–423. [PubMed: 20471243]
7. Pathania M, Yan LD, Bordey A. A symphony of signals conducts early and late stages of adult neurogenesis. Neuropharmacology. 2010; 58:865–876. [PubMed: 20097213]
8. Lin JHC, Takano T, Arcuino G, et al. Purinergic signaling regulates neural progenitor cell expansion and neurogenesis. Develop Biol. 2007; 302:356–366. [PubMed: 17188262]
9. Lacar B, Herman P, Hartman NW, et al. S phase entry of neural progenitor cells correlates with increased blood flow in the young subventricular zone. PLoS One. 2012; 7:e31960. [PubMed: 22359646]
10. Cao X, Li LP, Qin XH, et al. Astrocytic ATP release regulates the proliferation of neural stem cells in the adult hippocampus. Stem Cells. 2013; 31:1633–1643. [PubMed: 23630193]
11. Scemes E, Duval N, Meda P. Reduced expression of P2Y1 receptors in connexin43-null mice alters calcium signaling and migration of neural progenitor cells. J Neurosci. 2003; 23:11444–11452. [PubMed: 14673009]

NIH-PA Author Manuscript NIH-PA Author Manuscript NIH-PA Author Manuscript

12. Mishra SK, Braun N, Shukla V, et al. Extracellular nucleotide signaling in adult neural stem cells: Synergism with growth factor-mediated cellular proliferation. Development. 2006; 133:675–684. [PubMed: 16436623]
13. Striedinger K, Meda P, Scemes E. Exocytosis of ATP from astrocyte progenitors modulates spontaneous Ca^{2+} oscillations and cell migration. Glia. 2007; 55:652–662. [PubMed: 17309060]
14. Grimm I, Ullsperger SN, Zimmermann H. Nucleotides and epidermal growth factor induce parallel cytoskeletal rearrangements and migration in cultured adult murine neural stem cells. Acta Physiol. 2010; 199:181–189.
15. Weissman TA, Riquelme PA, Ivic L, et al. Calcium waves propagate through radial glial cells and modulate proliferation in the developing neocortex. Neuron. 2004; 43:647–661. [PubMed: 15339647]
16. Liu XX, HashimotoTorii K, Torii M, et al. The role of ATP signaling in the migration of intermediate neuronal progenitors to the neocortical subventricular zone. Proc Natl Acad Sci USA. 2008; 105:11802–11807. [PubMed: 18689674]
17. Liu X, Hashimoto-Torii K, Torii M, et al. Gap junctions/hemichannels modulate interkinetic nuclear migration in the forebrain precursors. J Neurosci. 2010; 30:4197–4209. [PubMed: 20335455]
18. Suyama S, Sunabori T, Kanki H, et al. Purinergic signaling promotes proliferation of adult mouse subventricular zone cells. J Neurosci. 2012; 32:9238–9247. [PubMed: 22764232]
19. Boccazzi M, Rolando C, Abbracchio MP, et al. Purines regulate adult brain subventricular zone cell functions: contribution of reactive astrocytes. Glia. 2014; 62:428–439. [PubMed: 24382645]
20. Khodosevich K, Zuccotti A, Kreuzberg MM, et al. Connexin45 modulates the proliferation of transit-amplifying precursor cells in the mouse subventricular zone. Proc Natl Acad Sci USA. 2012; 109:20107–20112. [PubMed: 23169657]
21. Zimmermann H, Zebisch M, Sträter N. Cellular function and molecular structure of ecto-nucleotidases. Purinergic Signal. 2012; 8:437–502. [PubMed: 22555564]
22. Braun N, Sévigny J, Mishra S, et al. Expression of the ecto-ATPase NTPDase2 in the germinal zones of the developing and adult rat brain. Eur J Neurosci. 2003; 17:1355–1364. [PubMed: 12713638]
23. Shukla V, Zimmermann H, Wang LP, et al. Functional expression of the ecto-ATPase NTPDase2 and of nucleotide receptors by neuronal progenitor cells in the adult murine hippocampus. J Neurosci Res. 2005; 80:600–610. [PubMed: 15884037]
24. Vandenbeuch A, Anderson CB, Parnes J, et al. Role of the ectonucleotidase NTPDase2 in taste bud function. Proc Natl Acad Sci USA. 2013
25. Mignone JL, Kukekov V, Chiang AS, et al. Neural stem and progenitor cells in nestin-GFP transgenic mice. J Comp Neurol. 2004; 469:311–324. [PubMed: 14730584]
26. Langer D, Hammer K, Koszalka P, et al. Distribution of ectonucleotidases in the rodent brain revisited. Cell Tissue Res. 2008; 334:199–217. [PubMed: 18843508]
27. Cooper-Kuhn CM, Kuhn HG. Is it all DNA repair? Methodological considerations for detecting neurogenesis in the adult brain. Brain Res Dev Brain Res. 2002; 134:13–21.
28. Braun N, Sévigny J, Robson SC, et al. Assignment of ecto-nucleoside triphosphate diphosphohydrolase-1/cd39 expression to microglia and vasculature of the brain. Eur J Neurosci. 2000; 12:4357–4366. [PubMed: 11122346]
29. Brun-Heath I, Ermonval M, Chabrol E, et al. Differential expression of the bone and the liver tissue non-specific alkaline phosphatase isoforms in brain tissues. Cell Tissue Res. 2011; 343:521–536. [PubMed: 21191615]
30. Bigonnesse F, Lévesque SA, Kukulski F, et al. Cloning and characterization of mouse nucleoside triphosphate diphosphohydrolase-8. Biochemistry USA. 2004; 43:5511–5519.
31. Lazarini F, Lledo PM. Is adult neurogenesis essential for olfaction? Trends Neurosci. 2011; 34:20–30. [PubMed: 20980064]
32. Steiner B, Klempin F, Wang L, et al. Type-2 cells as link between glial and neuronal lineage in adult hippocampal neurogenesis. Glia. 2006; 54:805–814. [PubMed: 16958090]

NIH-PA Author Manuscript NIH-PA Author Manuscript NIH-PA Author Manuscript

33. Jungenitz T, Radic T, Jedlicka P, et al. High-frequency stimulation induces gradual immediate early gene expression in maturing adult-generated hippocampal granule cells. Cereb Cortex. 2013 Epub ahead of print.
34. Sierra A, Encinas JM, Deudero JJP, et al. Microglia shape adult hippocampal neurogenesis through apoptosis-coupled phagocytosis. Cell Stem Cell. 2010; 7:483–495. [PubMed: 20887954]
35. Merz K, Herold S, Lie DC. CREB in adult neurogenesis - master and partner in the development of adult-born neurons? Eur J Neurosci. 2011; 33:1078–1086. [PubMed: 21395851]
36. Jagasia R, Steib K, Englberger E, et al. GABA-cAMP Response element-binding protein signaling regulates maturation and survival of newly generated neurons in the adult hippocampus. J Neurosci. 2009; 29:7966–7977. [PubMed: 19553437]
37. Ho CL, Yang CY, Lin WJ, et al. Ecto-nucleoside triphosphate diphosphohydrolase 2 modulates local ATP-induced calcium signaling in human HaCaT keratinocytes. PLoS One. 2013; 8:e57666. [PubMed: 23536768]
38. Melani A, Corti F, Stephan H, et al. Ecto-ATPase inhibition: ATP and adenosine release under physiological and ischemic in vivo conditions in the rat striatum. Exp Neurol. 2012; 233:193–204. [PubMed: 22001157]
39. Stafford MR, Bartlett PF, Adams DJ. Purinergic receptor activation inhibits mitogen-stimulated proliferation in primary neurospheres from the adult mouse subventricular zone. Mol Cell Neurosci. 2007; 35:535–548. [PubMed: 17553694]
40. Lacar B, Young SZ, Platel JC, et al. Gap junction-mediated calcium waves define communication networks among murine postnatal neural progenitor cells. Eur J Neurosci. 2011; 34:1895–1905. [PubMed: 22098557]
41. Messemer N, Kunert C, Grohmann M, et al. $P2X_7$ receptors at adult neural progenitor cells of the mouse subventricular zone. Neuropharmacology. 2013; 73C:122–137. [PubMed: 23727220]
42. Csölle C, Baranyi M, Zsilla G, et al. Neurochemical changes in the mouse hippocampus underlying the antidepressant effect of genetic deletion of $P2X_7$ receptors. PLoS One. 2013; 8:e66547. [PubMed: 23805233]
43. Delarasse C, Gonnord P, Galante M, et al. Neural progenitor cell death is induced by extracellular ATP via ligation of $P2X_7$ receptor. J Neurochem. 2009; 109:846–857. [PubMed: 19250337]
44. Kempermann G, Gast D, Kronenberg G, et al. Early determination and long-term persistence of adult-generated new neurons in the hippocampus of mice. Development. 2003; 130:391–399. [PubMed: 12466205]
45. Kempermann G, Kuhn HG, Gage FH. More hippocampal neurons in adult mice living in an enriched environment. Nature. 1997; 386:493–495. [PubMed: 9087407]
46. Fabel K, Wolf SA, Ehninger D, et al. Additive effects of physical exercise and environmental enrichment on adult hippocampal neurogenesis in mice. Front Neurosci. 2009; 3:50.10.3389/neuro.22.002.2009 [PubMed: 20582277]
47. Kobilo T, Liu QR, Gandhi K, et al. Running is the neurogenic and neurotrophic stimulus in environmental enrichment. Learn Mem. 2011; 18:605–609. [PubMed: 21878528]
48. Deisseroth K, Singla S, Toda H, et al. Excitation-neurogenesis coupling in adult neural stem/progenitor cells. Neuron. 2004; 42:535–552. [PubMed: 15157417]
49. Tashiro A, Sandler VM, Toni N, et al. NMDA-receptor-mediated, cell-specific integration of new neurons in adult dentate gyrus. Nature. 2006; 442:929–933. [PubMed: 16906136]
50. Lledo PM, Alonso M, Grubb MS. Adult neurogenesis and functional plasticity in neuronal circuits. Nat Rev Neurosci. 2006; 7:179–193. [PubMed: 16495940]
51. Domercq M, Vazquez-Villoldo N, Matute C. Neurotransmitter signaling in the pathophysiology of microglia. Front Cell Neurosci. 2013; 7:49. eCollection 2013. 10.3389/fncel.2013.00049 [PubMed: 23626522]
52. Koizumi S, Shigemoto-Mogami Y, Nasu-Tada K, et al. UDP acting at $P2Y_6$ receptors is a mediator of microglial phagocytosis. Nature. 2007; 446:1091–1095. [PubMed: 17410128]
53. Bulavina L, Szulzewsky F, Rocha A, et al. NTPDase1 activity attenuates microglial phagocytosis. Purinergic Signal. 2013; 9:199–205. [PubMed: 23208703]

NIH-PA Author Manuscript

NIH-PA Author Manuscript

NIH-PA Author Manuscript

54. Encinas JM, Michurina TV, Peunova N, et al. Division-coupled astrocytic differentiation and age-related depletion of neural stem cells in the adult hippocampus. Cell Stem Cell. 2011; 8:566–579. [PubMed: 21549330]

55. Bonaguidi MA, Wheeler MA, Shapiro JS, et al. In vivo clonal analysis reveals self-renewing and multipotent adult neural stem cell characteristics. Cell. 2011; 145:1142–1155. [PubMed: 21664664]

56. Dranovsky A, Picchini AM, Moadel T, et al. Experience dictates stem cell fate in the adult hippocampus. Neuron. 2011; 70:908–923. [PubMed: 21658584]

57. Song J, Zhong C, Bonaguidi MA, et al. Neuronal circuitry mechanism regulating adult quiescent neural stem-cell fate decision. Nature. 2012; 489:150–154. [PubMed: 22842902]

58. Steiner B, Kronenberg G, Jessberger S, et al. Differential regulation of gliogenesis in the context of adult hippocampal neurogenesis in mice. Glia. 2004; 46:41–52. [PubMed: 14999812]

NIH-PA Author Manuscript
NIH-PA Author Manuscript
NIH-PA Author Manuscript

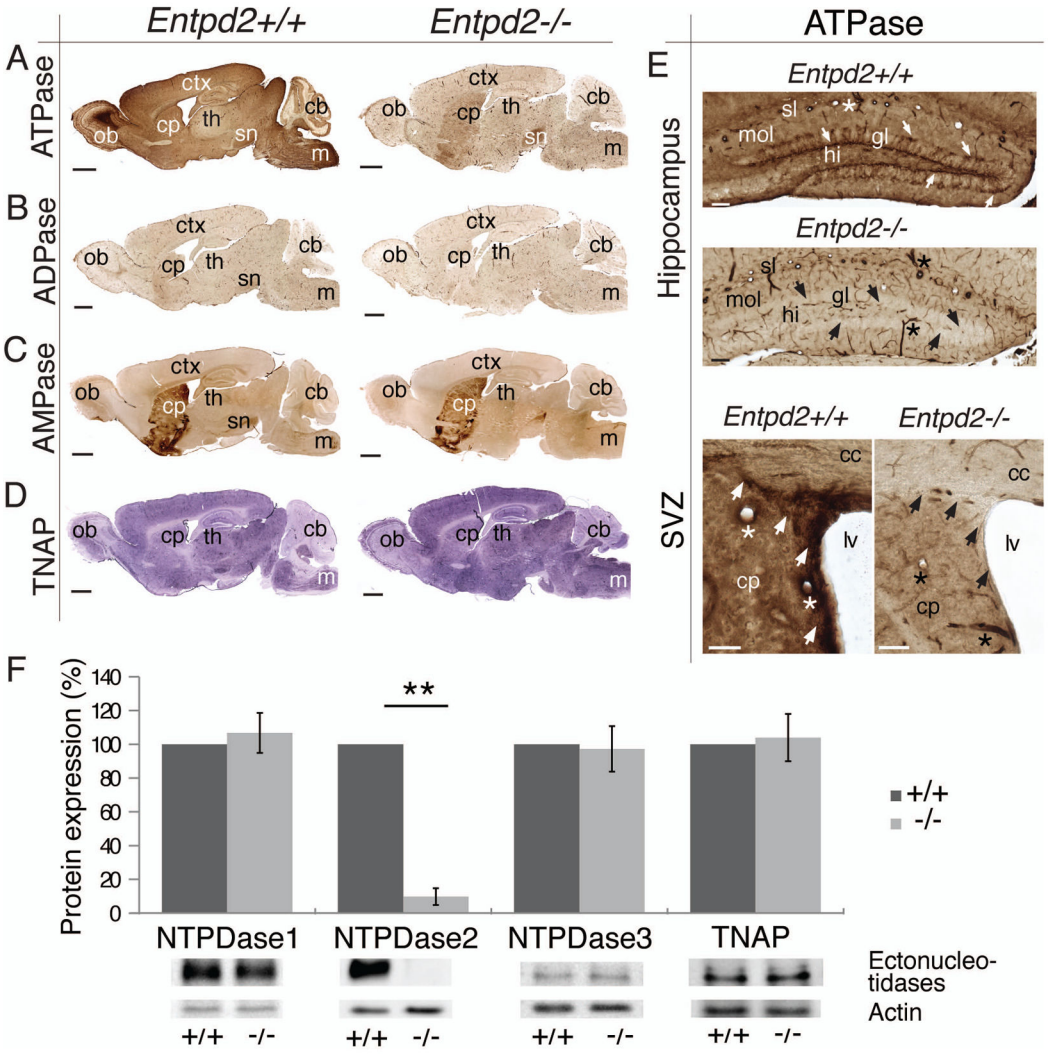

Figure 1.

Distribution of ectonucleotidase activity in WT and *Entpd2* KO mice. **(A–D)**: Enzyme histochemical reaction product in parasagittal sections using ATP, ADP and AMP as a substrate for visualizing ectonucleotidase activity and BCIP/NBT for alkaline phosphatase (TNAP) activity. **(E)**: Coronal sections of dentate gyrus (top) and the lateral ventricles (bottom). Arrows (top) depict the position of the radial type-1 cells and their ramifications that are intensely stained for ATPase activity in WT sections of the dentate gyrus and are not detectable in KO sections. Arrows (bottom) depict enhanced ATPase activity at the SVZ and its dorsal extension that is lost in *Entpd2* KO mice. Asterisks indicate NTPDase1-expressing blood vessels. **(F)**: Lack of upregulation of other ectonucleotidases in *Entpd2* KO mice as revealed by immunoblotting. Bar graph (mean ± SEM) represents quantitative analysis of immunoblots for NTPDase1 to NTPDase3 and TNAP in WT (+/+) and KO (−/−) mice. Actin served as a loading control. The apparent molecular masses (kDa) of the ectonucleotidases correspond to 72 (NTPDase1), 70 (NTPDase2), 75 (NTPDase3), and 75 (TNAP). n=10 mice for each condition. ** $p<0.01$, significant relative to control. cb, cerebellum; cc, corpus callosum; cp, caudoputamen; ctx, cerebral cortex; gl, granule cell

layer; hi, hilus; m, medulla oblongata; lv, lateral ventricle; mol, molecular layer; ob, olfactory bulb; sl, stratum lacunosum; sn substantia nigra; th, thalamus. (Scale bars, 500 μm, **A–D**; 100 μm, **E**)

NIH-PA Author Manuscript
NIH-PA Author Manuscript
NIH-PA Author Manuscript

NIH-PA Author Manuscript

NIH-PA Author Manuscript

NIH-PA Author Manuscript

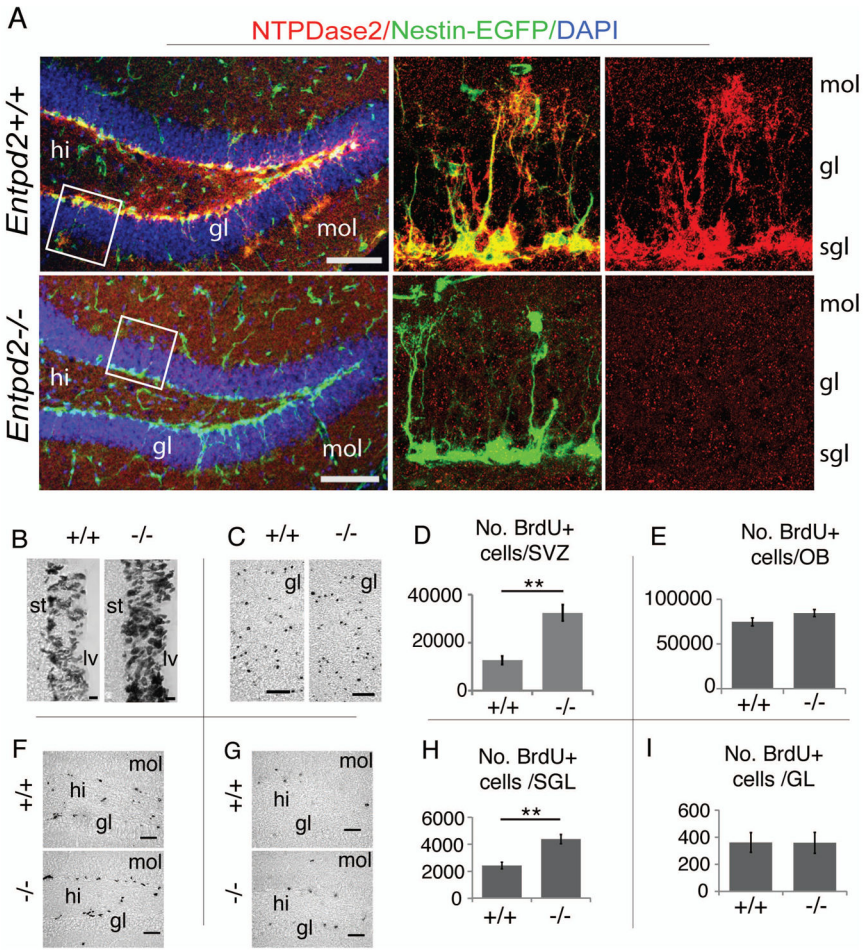

Figure 2.

Effect of *Entpd2* deletion on the structure of hippocampal type-1 cells and on the proliferation and survival of BrdU-labeled precursor cells. **(A)**: Dentate gyrus, overlay of fluorescence for nestin-EGFP (green) and immunostaining for NTPDase2 (red); DAPI staining (blue). The middle and right panels in **(A)** are blowups of regions indicated by white boxes. **(B,F)**: Immunostaining of SVZ **(B)** and dentate gyrus **(F)** for BrdU after five daily BrdU injections and analysis of mice 2 hours after the final injection. **(C,G)**: Corresponding immunostaining in the olfactory bulb **(C)** and dentate gyrus **(G)** 28 days after the final injection. **(D,E)**: Quantitative evaluation (mean ± SEM) of labeled cells corresponding to **(B)** and **(C)**, respectively (**D**, n=4–5 mice per condition; **E**, n=3–7 mice per condition). **(H,I)**: Quantitative evaluation (mean ± SEM) of labeled cells corresponding to (**F**) and (**G**), respectively (**H**, n= 4–10 mice per condition; **I**, n=5–10 mice per condition). ** $p<0.01$, significant to control. hi, hilus, gl, granule cell layer of hippocampus and olfactory bulb, respectively; lv, lateral ventricle; mol, molecular layer; sgl, subgranular layer; st, striatum. (Scale bars, 100 μm, **A**; 10 μm, **B**; 50 μm **C,F,G**)

NIH-PA Author Manuscript

NIH-PA Author Manuscript

NIH-PA Author Manuscript

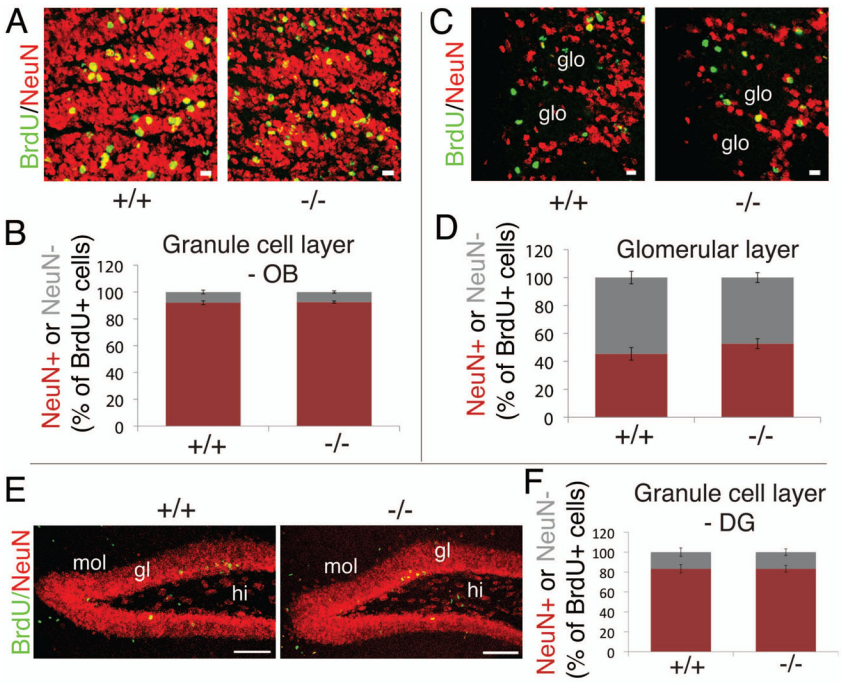

Figure 3.

Analysis of neuron formation in *Entpd2* +/+ and −/− mice 28 days after five daily BrdU injections. (**A,C,E)**: Immunostaining for BrdU (green) and NeuN (red) in the granule cell layer **(A)**, or glomerular layer of the olfactory bulb **(C)** and the dentate gyrus **(E). (B,D,F)**: Quantitative evaluation (mean ± SEM) of BrdU/NeuN double-labeled cells as depicted for **(A)**, **(C)** and **(E)**, respectively. 100% corresponds to the total number of BrdU-positive cells counted (100 and 50 BrdU+ cells counted per cell layer of the olfactory bulb and dentate gyrus, respectively) (**B**, n=5–6 mice per condition; **D**, n=5–6 mice per condition, **F**, n=3 mice per condition). Red, double-labeled cells; grey, cells labeled for BrdU only. gl, granule cell layer; glo, glomerulus; hi, hilus; mol, molecular layer (Scale bars, 10 μm **A,C**; 100 μm **E**).

NIH-PA Author Manuscript

NIH-PA Author Manuscript

NIH-PA Author Manuscript

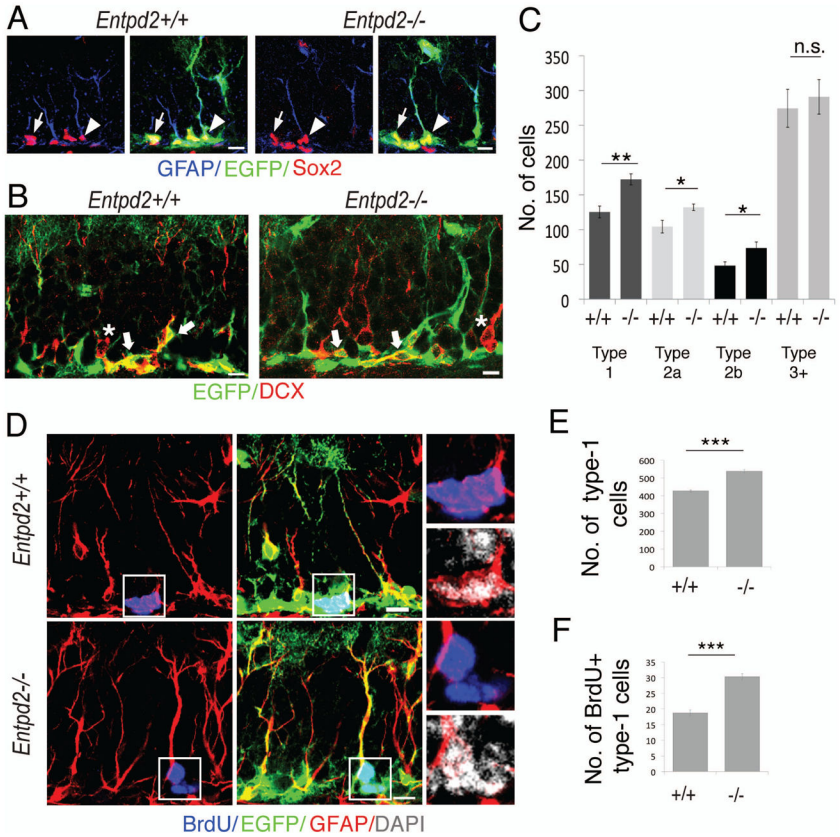

Figure 4.

Expansion of precursor cells in the subgranular zone of *Entpd2* +/+ and −/− mice. **(A,B)**: Analysis of fluorescence for nestin-EGFP (green), GFAP (blue), Sox2 (red) **(A)**, or nestin-EGFP (green) and DCX (red) **(B)**. Cell types were differentiated as follows: type-1 (expressing nestin-EGFP and immunopositive for GFAP and Sox2 and showing at least a short process facing the granule cell layer) (arrow heads in **A**), type-2a (expressing nestin-EGFP and immunopositive for Sox2) (arrows in **A**), type-2b (expressing nestin-EGFP and immunopositive for DCX (thick arrows in **B**), type-3+ (immunopositive for DCX but lacking the other markers (asterisks in **B**). **(C)**: Corresponding abundance (total number of cells, four sections per animal) of individual cell types in WT (+/+) and KO (−/−) animals (n=9). **(D-F)**: Increased proliferation of type-1 cells. **(D)**: 2 hours after the final BrdU injection (3 pulses at 2 hour interval) animals were perfused and proliferating type-1 cells were identified by labeling for BrdU (blue), EGFP (green), GFAP (red) and DAPI (grey). Left images: double labeling for BrdU and GFAP; middle images: triple labeling for BrdU, EGFP and GFAP. The boxed regions are enlarged on the right hand side and include labeling for DAPI. For clarity, labeling for only GFAP and BrdU or GFAP and DAPI is presented. Note overlap of labeling for BrdU and DAPI. **(E)**: Total number of type-1 cells (10 sections per animal) in WT (+/+) and KO (−/−) animals (n=7). **(F)**: Total number of BrdU-labeled type-1 cells (10 sections per animal) in WT (+/+) and KO (−/−) animals (n=7). Bar graphs are mean ± SEM. *p<0.05, **p<0.01; ***p<0.001, significant relative to control, n.s., difference not significant. (Scale bars, 10 μm, **A,B,D**)

NIH-PA Author Manuscript

NIH-PA Author Manuscript

NIH-PA Author Manuscript

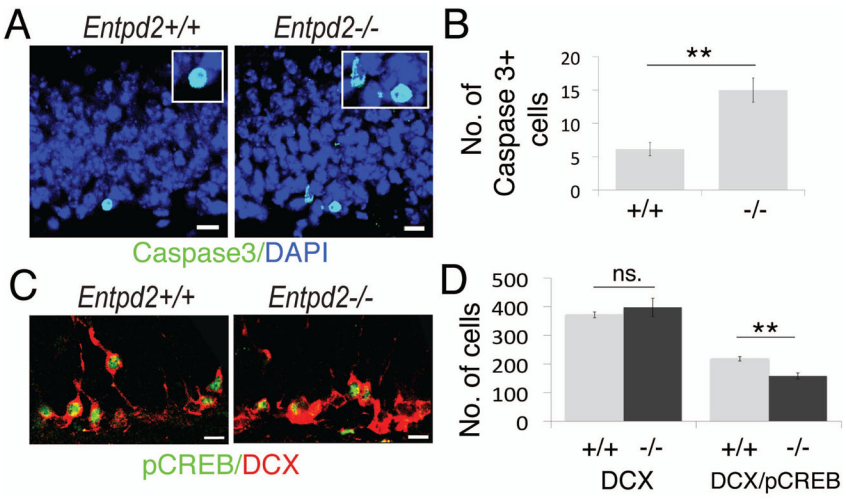

Figure 5.

Analysis of apoptosis and immunofluorescence for pCREB. (**A**): Immunofluorescence for activated caspase-3 (green); DAPI, blue. Boxed regions: enlarged images of caspase-3-labeled cells **(B)**: Corresponding quantification of caspase-3-positive cells in the SGL of WT (+/+) (n=7) and KO (−/−) (n=6) animals. **(C)**: Immunofluorescence for pCREB (green) and DCX (red) in the SGL. **(D)**: Corresponding quantification of DCX-positive cells (left bars) and pCREB-labeled DCX-positive cells (right bars) in WT (+/+) (n=7) and KO (−/−) (n=5) animals. Bar graphs are mean ± SEM. ***p*<0.01, significant relative to control, n.s., difference not significant. (Scale bars, 10 μm, **A,C**)

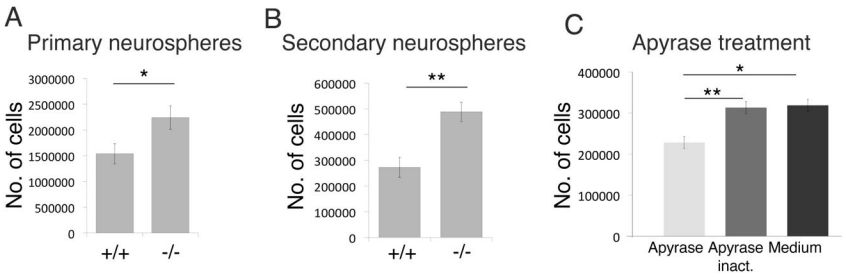

Figure 6.

Differential in vitro progenitor cell proliferation in *Entpd2* +/+ and −/− mice. **(A,B)**: Total cell numbers determined in primary **(A)** and secondary **(B)** neurospheres, respectively (n=3). **(C)** Total cell numbers after addition of apyrase (1 U/ml) to secondary neurospheres from of *Entpd2* KO mice as compared to addition of heat inactivated apyrase or a corresponding volume of culture medium (n=6). Bar graphs are mean ± SEM. **p*<0.05, ***p*<0.01, significant relative to control.

NIH-PA Author Manuscript NIH-PA Author Manuscript NIH-PA Author Manuscript